CAMBRIDGE JOURNALS

Proof Delivery Form

MRS Bulletin

Date of delivery: 11.08.2020

Journal and vol/article ref: mrs MRS2000226

Number of pages (not including this page): 8

This proof is sent to you on behalf of Cambridge University Press. Please check the proofs carefully. Make any corrections necessary on a hardcopy and answer queries on each page of the proofs

Please return the **marked proof** within 2 days of receipt to:

Authors are strongly advised to read these proofs thoroughly because any errors missed may appear in the final published paper. This will be your ONLY chance to correct your proof. Once published, either online or in print, no further changes can be made.

To avoid delay from overseas, please send the proof by airmail or courier.

If you have **no corrections** to make, please email lwilson@mrs.org; oldham@mrs.org to save having to return your paper proof. If corrections are light, you can also send them by email, quoting both page and line number.

- The proof is sent to you for correction of typographical errors only. Revision of the substance of the text is not permitted, unless discussed with the editor of the journal. Only **one** set of corrections are permitted.
- Please answer carefully any author queries.
- Corrections which do NOT follow journal style will not be accepted.
- A new copy of a figure must be provided if correction of anything other than a typographical error introduced by the typesetter is required.

- If you have problems with the file please contact mrs_cuppm@novatechset.com

Please note that this pdf is for proof checking purposes only. It should not be distributed to third parties and may not represent the final published version.

Important: you must return any forms included with your proof. We cannot publish your article if you have not returned your signed copyright form.

NOTE - for further information about **Journals Production** please consult our **FAQs** at http://journals.cambridge.org/production_faqs

Author Queries

Journal: MRS Bulletin

Manuscript: S0883769420002262jra

Q1	The distinction between surnames can be ambiguous, therefore to ensure accurate tagging for indexing purposes online (e.g. for PubMed entries), please check that the highlighted surnames have been correctly identified, that all names are in the correct order and spelt correctly.

In situ electrochemical scanning/transmission electron microscopy of electrode–electrolyte interfaces

Raymond R. Unocic, Katherine L. Jungjohann, B. Layla Mehdi, Nigel D. Browning, and Chongmin Wang

Q1

Insights into the dynamics of electrochemical processes are critically needed to improve our fundamental understanding of electron, charge, and mass transfer mechanisms and reaction kinetics that influence a broad range of applications, from the functionality of electrical energy-storage and conversion devices (e.g., batteries, fuel cells, and supercapacitors), to materials degradation issues (e.g., corrosion and oxidation), and materials synthesis (e.g., electrodeposition). To unravel these processes, *in situ* electrochemical scanning/transmission electron microscopy (ec-S/TEM) was developed to permit detailed site-specific characterization of evolving electrochemical processes that occur at electrode-electrolyte interfaces in their native electrolyte environment, in real time and at high-spatial resolution. This approach utilizes "closed-form" microfabricated electrochemical cells that couple the capability for quantitative electrochemical measurements with high spatial and temporal resolution imaging, spectroscopy, and diffraction. In this article, we review the state-of-the-art instrumentation for *in situ* ec-S/TEM and how this approach has resulted in new observations of electrochemical processes.

Introduction

Characterizing dynamic electrochemical processes directly within the liquid phase and under realistic working conditions has long been desired by researchers interested in understanding the nanoscale mechanisms and kinetics of interfacial electrochemical reactions. There has been significant progress in the development of specialized electrochemical cells that can be used in conjunction with x-ray and neutron diffraction, scanning probe microscopy, Raman spectroscopy, x-ray absorption spectroscopy, and x-ray photoelectron spectroscopy techniques.[1] However, most of these techniques are limited in spatial and temporal resolution, and in the type of information that can be extracted (e.g., lattice expansion, crystallography, electronic structure, or surface chemistry). The scanning/transmission electron microscope (S/TEM) on the other hand, has the advantage of several characterization modalities combined in one instrument: high spatial and temporal resolution imaging, chemical analysis (electron energy loss spectroscopy [EELS] and energy dispersive x-ray spectroscopy [EDS]), and structure/phase identification (electron diffraction).[2]

Microfabricated electrochemical liquid cells designed specifically for S/TEM have enabled quantitative electrochemical measurements to be conducted simultaneously with detailed structural and chemical analysis in the technique termed *in situ* electrochemical scanning transmission electron microscopy (ec-S/TEM).[3,4] The breakthroughs in performing electrochemical experiments *in situ* resulted from development of small form-factor electrochemical cells and specialized *in situ* TEM holders with integrated electrical biasing contacts, see **Figure 1**a. Microfabrication techniques, standard to the semiconductor industry, provide methods for fabricating paired microchips that support mechanically and chemically robust, electron-transparent Si_3N_4 viewing membranes for imaging, see Figure 1b.[5–7] Additional features such as working, counter, and reference electrodes with lithographically patterned spacers (~~e.g., SU-8 photoresist or gold~~) provide electrical circuitry and isolation, respectively, for electroanalytical measurements with electrode connection to an external potentiostat.

Modern *in situ* S/TEM holders include integrated microfluidic tubing connected to an external syringe pump for

Raymond R. Unocic, Center for Nanophase Materials Sciences, Oak Ridge National Laboratory, USA; unocicrr@ornl.gov
Katherine L. Jungjohann, Center for Integrated Nanotechnologies, Sandia National Laboratories, USA; kljungj@sandia.gov
B. Layla Mehdi, Albert Crewe Center for Electron Microscopy, University of Liverpool, UK; ~~b.l.mehdi@liverpool.ac.uk~~
Nigel D. Browning, Albert Crewe Center for Electron Microscopy, University of Liverpool, UK; nigel.browning@liverpool.ac.uk
Chongmin Wang, Pacific Northwest National Laboratory, USA; Chongmin.wang@pnnl.gov
doi:10.1557/mrs.2020.226

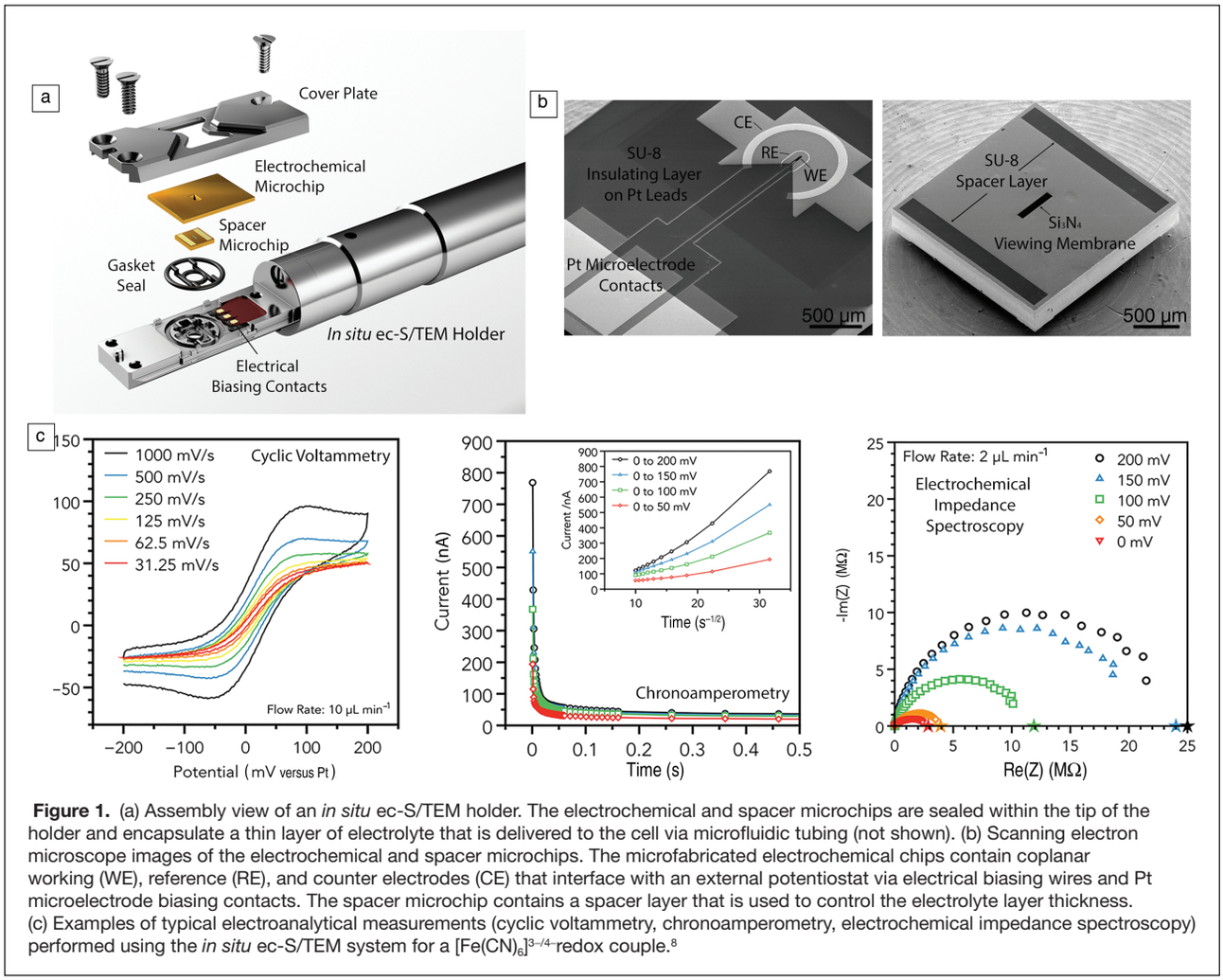

Figure 1. (a) Assembly view of an *in situ* ec-S/TEM holder. The electrochemical and spacer microchips are sealed within the tip of the holder and encapsulate a thin layer of electrolyte that is delivered to the cell via microfluidic tubing (not shown). (b) Scanning electron microscope images of the electrochemical and spacer microchips. The microfabricated electrochemical chips contain coplanar working (WE), reference (RE), and counter electrodes (CE) that interface with an external potentiostat via electrical biasing wires and Pt microelectrode biasing contacts. The spacer microchip contains a spacer layer that is used to control the electrolyte layer thickness. (c) Examples of typical electroanalytical measurements (cyclic voltammetry, chronoamperometry, electrochemical impedance spectroscopy) performed using the *in situ* ec-S/TEM system for a $[Fe(CN)_6]^{3-/4-}$ redox couple.[8]

controlled delivery and flow of electrolytes, whilst earlier designs used a syringe to introduce electrolyte into an etched entry port between the chips for static fluid experiments. To form the electrochemical cell, paired microchips (electrochemical and spacer microchips) were either glued, wafer bonded, or clamped together, and then placed within the holder. While the overall size scale, geometric electrode layout, and electrode material selection have evolved over time, the basic design concepts have remained the same. For the development of any new technique, it is important to benchmark capabilities; several studies[8–10] have demonstrated the feasibility of performing electroanalytic measurements such as cyclic voltammetry (CV), chronoamperometry, and electrochemical impedance spectroscopy within these microfabricated electrochemical cell, examples of which are shown in Figure 1c for a $[Fe(CN)_6]^{3-/4-}$ redox couple.

Electrodeposition: Nucleation and growth mechanisms

The motivation for the development of *in situ* ec-S/TEM was to study the mechanisms of Cu electrodeposition for integrated circuits. The earliest *in situ* electrochemical experiments clearly demonstrated the power of this technique, as in the case of directly imaging Cu nanoparticle nucleation and growth during galvanostatic electrodeposition from a $CuSO_4$ electrolyte.[6] Individual nanoparticle growth kinetics were correlated with current-time transient measurements through time-resolved TEM imaging with nanometer-scale resolution and results were compared with well-established theories of diffusion-limited nanoparticle growth to better understand the nanoparticle growth mechanisms.[11]

Similar studies have followed, such as the electrochemical deposition of metals *in situ*, to obtain new insights into the factors that control morphological changes at the electrode/electrolyte interface.[12–14] For example, the electrodeposition of Ni thin films from an aqueous $NiCl_2$ electrolyte was found to be the result of anisotropic nucleation of Ni crystals ahead of the growth front,[15] and growth instabilities at the solid-liquid interface resulting in planar or dendritic growth were found to be dependent upon the magnitude of potential changes (**Figure 2**),[16] electrolyte concentration,[17] and chemical additives.[18] Furthermore, STEM imaging as opposed to TEM,

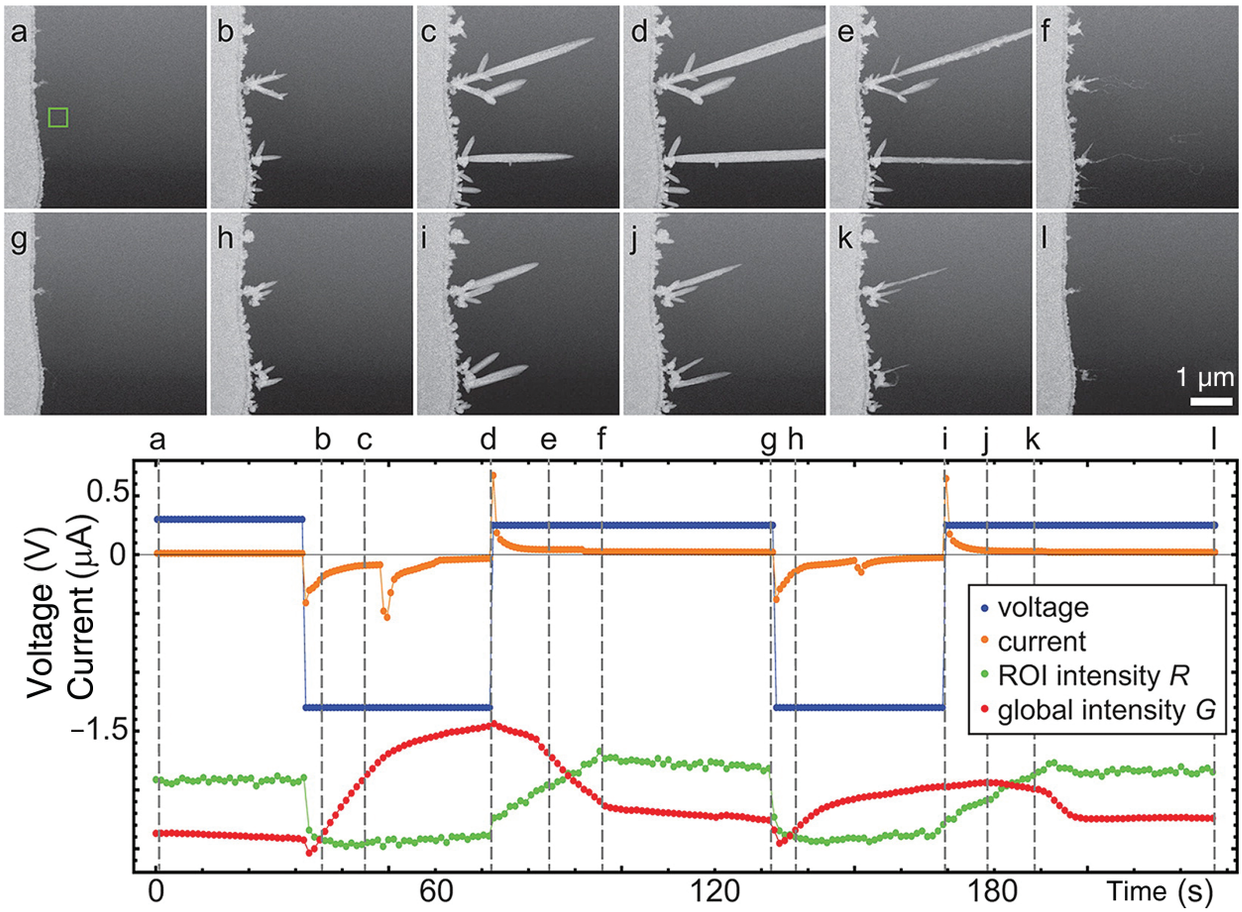

Figure 2. Scanning transmission electron microscopy imaging of repeated Pb dendrite growth and collapse during electrochemical cycling from a $Pb(NO_3)_2$ electrolyte on a Au working electrode. (a–f) and (g–1) are taken from consecutive cycles, with the individual frame times indicated on the current-voltage and region of interest (ROI) and global intensity plot below. Reprinted with permission from Reference 16. © 2012 American Chemical Society.

can be used to chemically map ion concentration gradients to improve understanding of diffusional processes at evolving electrochemical interfaces.[16] It is worth noting here that these few examples present a nanoscale view of nanoparticle and dendrite growth mechanisms, which could not otherwise have been observed with any other experimental method.

Electrochemical energy storage

Rechargeable batteries represents one of the major energy-storage solutions for mobile and stationary applications. In a simplistic view, the operating principle of rechargeable batteries relies upon the reversible shuttling of ions via the electrolyte between the anode and cathode during charge and discharge cycling. One of the central goals for rechargeable battery research is to establish the direct correlation between electrochemical battery performance and structural/chemical evolution of electrode–electrolyte interfaces during cycling. The *in situ* ec-S/TEM technique has greatly impacted energy storage research by enabling studies of the solid electrolyte interphase (SEI) formation, Li metal dendrite growth, interfacial reactions in metal-air batteries, and phase changes during ion intercalation, alloying, or conversion reactions.

The SEI is a passivating interfacial film that forms as a consequence of interfacial reactions between the electrode and electrolyte[19–21] and is critical to the performance of rechargeable batteries. A better understanding of SEI formation mechanisms and film evolution is essential for tailoring better batteries with improved cycling durability and performance. Silicon is a representative anode case that involves Li^+ ion alloying-induced volumetric changes and provides an opportunity to monitor the response of the SEI to electrode volumetric changes, which was studied with *in situ* ec-S/TEM.[22] Correlation between the electrochemical properties with Si volume change upon lithiation (Li alloying) was reported; however, the SEI film observation was not achieved due to imaging spatial resolution limitations through the electrolyte. With an improved cell design, SEI formation on graphitic[23] and Ti[24] anodes were observed.

Remarkably, EDS has been used to reveal the chemical composition of the SEI layer (C, O, and F); electron

nanodiffraction analysis revealed the existence of LiF nanocrystals in the SEI layer,[24] which was further confirmed by subsequent studies.[25,26] *In situ* high-spatial-resolution TEM imaging, coupled with real-time quantitative electrochemistry, was also performed, which tracked SEI formation on a Au working electrode using a standard $LiPF_6$-ethylene carbonate/dimethyl carbonate (EC/DMC) organic electrolyte and revealed that the SEI film was not uniform, but instead followed the Li dendrite morphology.[27] The thickness and density of the SEI layer as a function of sweeping potential has also been studied, revealing that the SEI was approximately twice as dense as the electrolyte based on quantitative imaging analysis, which informs the true nature of the SEI layer in structure and chemistry.[28]

Unraveling Li dendritic growth mechanisms using *in situ* ec-S/TEM has also been pursued in the past few years. Metallic anodes, such as Li, have a much higher capacity, yet during operation, metal stripping and redeposition typically occurs nonuniformly, resulting in dendrite growth upon repeated cycling. Lithium dendrites are known to cause short-circuiting between the anode and cathode, leading to battery failure. The dynamic processes of lithium dendrite growth and electrolyte decomposition in the electrochemical lithiation and delithiation of Au anodes from a commercial $LiPF_6$-ethylene carbonate/diethyl carbonate (EC/DEC) electrolyte has been reported in one study.[26] In this work, Li dendrite growth and dissolution was monitored to understand the formation of "dead" Li that is detached from the electrode during cycling. Considering the low volumetric density of Li metal, interpreting the contrast difference between the SEI layer and Li metal deposition can be challenging. As previously mentioned, S/TEM imaging can be used to clearly distinguish changes in chemical composition. Since the Li metal density is below that of the surrounding electrolyte and the Si_3N_4 windows, a contrast reversal is observed for Li metal between high-angle annular dark-field (HAADF) and bright-field (BF)-STEM images, allowing Li to be identified from Li-containing compounds.[29–32]

Li nucleation, growth, and shrinkage in a confined liquid cell also depends on the overpotential; Li growth can occur either at the dendrite base or tip.[33] The presence of trace amounts of H_2O, at the ppm level, yields clear morphological changes in the Li dendrites, as shown in **Figure 3**.[34] These observations further demonstrate that the rate of SEI formation can control Li growth either from the base or tip, with the former linked to an intermittent growth, leading to kinked segments of a nearly constant diameter Li dendrite. More globular and faceted morphology of Li dendrites[28] appear to be consistent with *ex situ* cryogenic-TEM observations,[35,36] where Li dendrites in carbonate-based electrolytes grew along the [111], [110], or [211] directions as faceted, single-crystalline nanowires.[35]

Metal-air batteries, typically metallic anode (Li^+, Na^+, and K^+) paired with O_2 and the cathode, represent another category

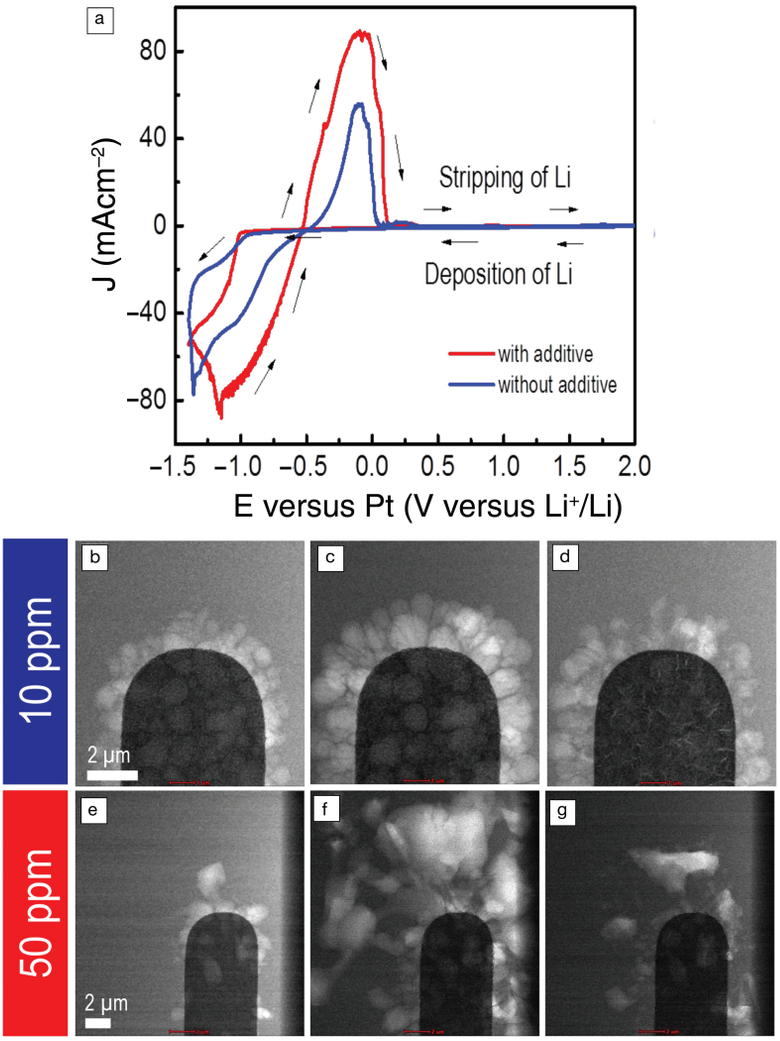

Figure 3. (a) Cyclic voltammograms obtained from an *operando* ec-S/TEM cell showing charge-discharge cycling from a Pt electrode in 1M $LiPF_6$ in propylene carbonate electrolyte with 10 and 50 ppm additions of H_2O. (b–d) Bright-field (BF) images showing the deposition/stripping of Li for the electrolyte without additives (i.e., 10 ppm residual H_2O), (b) at the start of the deposition, (c) at the peak of the deposition, and (d) after discharge is completed. (e–g) BF images showing the same for the electrolyte containing an addition of 50 ppm H_2O.[34]

of high-capacity electrochemical energy-storage systems for which *in situ* ec-S/TEM experiments have been conducted. These systems are highly complex as the principal operation of metal-air battery is based on the reversible formation and oxidation of their discharge products (e.g., lithium peroxide Li_2O_2 [Li-O_2 battery] and NaO_2 [Na-O_2 battery]) at the cathode surface. However, the formation of these main interfacial discharge products is not yet fully understood and involves multistep reactions taking place both in solution as well as at the electrode/electrolyte interface. For example in the Na-O_2 system, the formation of highly soluble NaO_2 cubes during reduction is a solution-mediated nucleation process, while the previously unknown oxidation of NaO_2, was found to proceed via a solution mechanism.[21] On the other hand the Li-O_2 system, exhibits significant challenges which limit their application such as low rate capacity, limited charge-discharge cycling due to decomposition of both the electrolyte and the electrode materials during the oxygen reduction and evolution, and poor solubility of Li_2O_2 as the main discharge product. This leads to increased overpotential and fast capacity fading during cycling.[37]

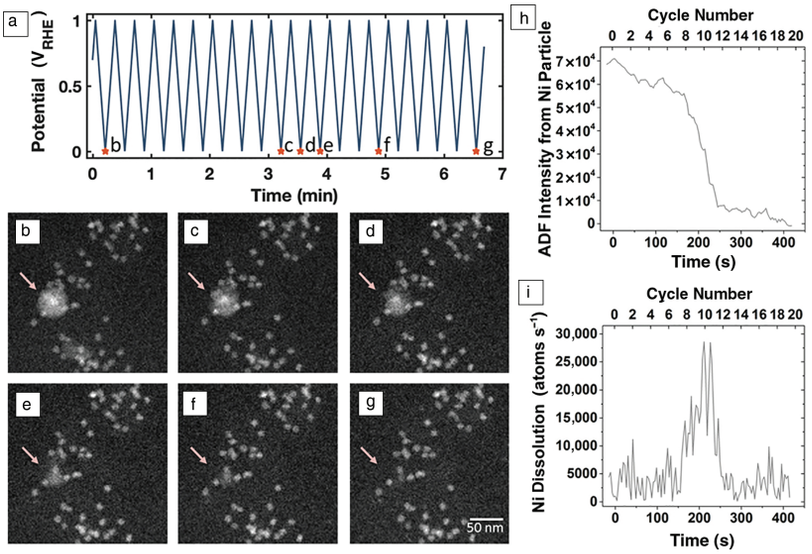

Figure 4. High-angle annular dark-field (ADF) scanning transmission electron microscopy *in situ* imaging of the catalyst structure during electrochemical potential cycling between 0.0 and +1.0 V_{RHE} in 0.1 M $HClO_4$ for 20 CV cycles with 100 mV s^{-1} sweep rate. (a) Potential profile over time with marked points corresponding to the images below. (b–g) A Ni-rich particle marked by the arrow disappears during cycling, first becoming less dense, then spongy, and finally dissolving completely. (h) ADF intensities of the Ni-rich particles over time during potential cycling and (i) the resulting Ni dissolution rate. Reprinted with permission from Reference 42. © 2019 Royal Society of Chemistry.

Cathode structural stability and cathode-electrolyte interfaces may be explored using a combination of electron diffraction, EELS, and imaging. Electron diffraction tomography can be used to determine the atomic coordinates, site occupancies (including lithium occupancy), and cell parameters of $LiFePO_4$ cathode during electrochemical cycling in a liquid electrolyte.[38] Similarly, Li-ion transport kinetics and degradation mechanisms in $LiFePO_4$ particles were studied during charge/discharge cycling, leading to *in situ* determination of the lithiation state for a $LiFePO_4$ electrode and the surrounding aqueous electrolyte in real time, with nanoscale resolution imaging.[39]

Electrocatalysis

Fuel cells are an important energy-conversion technology that uses electrocatalysts for the cathodic oxygen reduction reaction and anodic hydrogen oxidation reaction to generate electrical energy. To better design electrocatalysts with high activity, selectivity, and durability, an understanding of how the catalysts behave during operation is needed. Catalyst dissolution, coarsening, dealloying, reshaping, and support corrosion can lead to a decline in performance.[40] Direct observations of the coarsening behavior of a Pt-Fe electrocatalyst were linked to the cell potential via CV measurements in 0.1M $HClO_4$ at 10 mV/s.[41] Electrochemical potential cycling of carbon-supported Pt-Ni electrocatalysts in 0.1M $HClO_4$, for multiple CV cycles and between voltage ranges up to 1.4 V_{RHE}, revealed new observations of electrocatalyst coalescence, Ni-rich particle dissolution, carbon support corrosion and overall morphological changes, as shown in **Figure 4**.[42] These studies enabled new insight regarding electrocatalyst degradation mechanisms *in situ* ec-S/TEM.

Materials degradation

Corrosion is the most prominent degradation mechanism in metals, with widespread impact on our economy in terms of infrastructure, transportation, aerospace, and energy harvesting.[43] The scientific need for a fundamental understanding of corrosion initiation mechanisms is high; however, the experimental techniques required to extract quantitative structural and compositional information from nanoscale solid–liquid interfaces are limited. *In situ* liquid-cell and ec-S/TEM capabilities[3] have recently been used to investigate metal solid–liquid interfaces to provide insights into the characteristics of localized corrosion. S/TEM imaging provides a simultaneous view of grains and grain boundaries in metals,[44] as these are the dominant microstructural features that influence the initiation sites of localized corrosion.

An example is shown in **Figure 5**, where BF STEM images capture the loss of cementite grains in an iron matrix during exposure of 1018 low-carbon steel to a 5 ppm H_2S aqueous solution. These *in situ* S/TEM studies identified many common corrosion characteristics that link nanoscale observations to bulk corrosion behavior. Corrosion phenomena observed

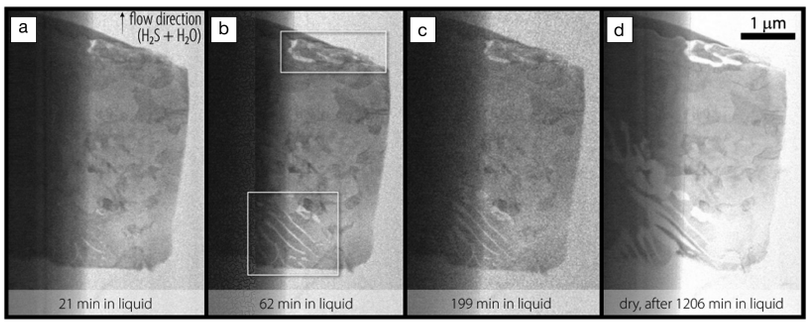

Figure 5. *In situ* scanning transmission electron microscopy corrosion of 1018 low-carbon steel in a 5 ppm H_2S aqueous solution, identified the preferential loss of cementite from the iron matrix, with an overall conversion of the lamella into an iron oxide corrosion product. (b) Showcases the development of two galvanic reactions, the top rectangular box encloses the preferential reaction between the Pt/C coating against the steel, and the bottom box indicates the removal of cementite from the ferrite matrix.[1]

using *in situ* S/TEM include fractal patterns,[45–49] blisters,[46,47] dealloying at grain boundaries,[50] inclusion dissolution,[51] pits,[47] galvanic coupling,[52] and stress-corrosion cracking.[53] New microelectromechanical designs allow for quantitative *in situ* S/TEM of coupled electrochemical and mechanical processes,[54] such as stress-corrosion cracking. Static solution or microfluidic capabilities can be designed into the corrosion experiments, depending on the specimen holder design or epoxy-sealed platform used. Microfluidic control over the corrosive solution allows for rapid changes in solution chemistry as well as the evacuation of the solution to provide reduced background noise for compositional mapping. Additionally, information regarding the corrosion rate, specimen thickness changes,[52] and corrosion product species[51] can be identified using *in situ* S/TEM. Although the electron beam is known to significantly impact the pH and chemistry of the corrosive solution, mitigation strategies can reduce this impact, though generally the impact of the beam limits the spatial resolution for imaging to the nanoscale.

Corrosion can also be controlled using ec-S/TEM for electrochemical analysis of the reaction.[51] Careful attachment of the specimen to an electrode is required for ec-S/TEM, but this could introduce a known artifact arising from the possible galvanic coupling between the specimen and electrode. The galvanic coupling may drive the corrosion reaction of two materials in contact that have different electronic potentials.[52] Specimens designed for electron transparency will be susceptible to this effect; therefore, overcoming this artifact must be designed into the specimen attachment protocol for electrochemical contact.[51] *In situ* ec-S/TEM studies of battery electrodes have visualized corrosion events, or self-discharge of metal deposits, that may arise due to this galvanic coupling artifact.[32] Future *in situ* ec-S/TEM and corrosion studies will benefit from (1) improved specimen preparation methods that reduce artifacts and improve electrical connections,[55] (2) the addition of temperature control to the solution,[56] and (3) high-speed chemical analysis from the solid-liquid interface during the reaction.[57]

Mitigating electron-beam-induced artifacts

The influence of the electron beam poses another challenge that sometimes causes undesirable beam–matter interactions such as radiolysis, electrolyte degradation and redox reactions.[58] Understanding these effects is important for *in situ* ec-S/TEM experiments, and strategies to mitigate e-beam artifacts such as low-dose imaging have been reported.[59,60] Specific to organic electrolytes used in Li-ion batteries ($LiPF_6$ in EC/DMC), it was reported that imaging with the electron beam can break down the solvent into gaseous products and the $LiPF_6$ to LiF. Additionally, the SEI layers were found to be sensitive to high-energy electron beams.[61] Strategically, the use of scavenger species that react with solvated electrons has been demonstrated to be a viable approach for mitigating possible modification of electrochemical processes by imaging with the electron beam.[62] On the other hand, effects of the electron beam on the electrochemical process itself remain largely unknown. Some calibration experiments indicate that the electron beam may not significantly modify the electrochemical process,[8,39] but more detailed studies are needed.

Improved cell design and quantitative measurements

Another major gap that currently exists for the *in situ* ec-S/TEM technique is replication of bulk electrochemical testing.[63] This gap is inherent to the microfabricated electrochemical cells that have the requirements to fit within the small pole piece gap of the TEM (typically several millimeters). By miniaturizing the electrochemical cell diffusion profiles, the current distribution and electric field gradients become different from those of bulk tests due to the limited electrolyte volume (with thickness less than a micron), microelectrode size-scale, and geometrical layout.[64] Typically, two or three coplanar microelectrodes are microfabricated in either a linear or concentric configuration, which is a significant deviation from stacked electrodes used in bulk coin cells for batteries, as an example. The electric-field distribution on the working electrode is influenced by the relative positioning of the electrodes in the cell, where a nonuniform electric field gradient may lead to localized hot spots, that can subsequently drive localized electrochemical reactions.[29] Electrolyte concentration can also vary during a reaction, and therefore, careful design of experiments under electrolyte flow versus static conditions needs to be determined, since this will affect the electrochemical data. These compounding issues may lead to significant differences that need to be fully understood in order for the electroanalytical data to be analyzed and interpreted properly.

Summary

In situ ec-S/TEM has been shown to be a powerful high-resolution method that provides unique insights into dynamically evolving electrochemical reactions at electrode-electrolyte interfaces. This technique has already had impact on diverse fields, including electrodeposition, energy-storage, catalysis, and liquid-phase corrosion. Emerging S/TEM capabilities focused on increased signal content (spatial and temporal resolution, sensitivity) for lower dose imaging,[65] increased accessibility for signal detection at high resolution,[66] advanced spectroscopy and diffraction methods,[67] coupled with platform developments for improved environmental control, microfluidic exchange, and specimen stability, promise to expand the applications of these methods even further in the near future. While the inherent physics and chemistry of both the imaging mechanism and sample process being observed may never allow us to achieve the same routine resolution afforded by aberration-corrected S/TEM observations of electron-beam stable materials under high-vacuum conditions, the correlated imaging, diffraction, and spectroscopy observations obtained from *in situ* experiments will continue to provide unique insights into key phenomena, and a fundamental basis for improved simulations, predictive modeling and process design for next-generation energy-storage, electrocatalytic, and corrosion-resistant materials.

Acknowledgments

Research supported by the Center for Nanophase Materials Sciences (RRU) at Oak Ridge National Laboratory and the Center for Integrated Nanotechnologies (KLJ) at Sandia National Laboratory, which are US Department of Energy (DOE) Office of Science User Facilities. Sandia National Laboratories is a multi-mission laboratory managed and operated by National Technology and Engineering Solutions of Sandia, LLC, a wholly owned subsidiary of Honeywell International, Inc., for the US DOE's National Nuclear Security Administration under Contract No. DE-NA-0003525. The views expressed in the article do not necessarily represent the views of the US DOE or the United States Government. B.L.M. and N.D.B. acknowledge support for this work from the UK Faraday Institution's Degradation, Recycling and Characterization projects. In addition, aspects of this work were supported by the Joint Center for Energy Storage Research (JCESR), an Energy Innovation Hub funded by the US DOE, Office of Science, Basic Energy Sciences and by the Chemical Imaging Initiative, a Laboratory Directed Research and Development Program at Pacific Northwest National Laboratory (PNNL). Support was also provided by the Assistant Secretary for Energy Efficiency and Renewable Energy, Office of Vehicle Technologies of the US DOE under the Advanced Battery Materials Research (BMR) Program (CMW). Work at PNNL was conducted at the William R. Wiley Environmental Molecular Sciences Laboratory (EMSL), a national scientific user facility sponsored by US DOE Office of Biological and Environmental Research. PNNL is operated by Battelle for the Department of Energy under Contract No. DE-AC05–76RL01830.

References

1. A.M. Tripathi, W.N. Su, B.J. Hwang, *Chem. Soc. Rev.* **47**, 736 (2018).
2. S.J. Pennycook, P.D. Nellist, *Scanning Transmission Electron Microscopy* (Springer, New York, 2011).
3. F.M. Ross, *Science* **350**, aaa9886-1 (2015).
4. F.M. Ross, *Liquid Cell Electron Microscopy* (Cambridge University Press, Cambridge, UK, 2017).
5. J.M. Grogan, H.H. Bau, *J. Microelectromech. Syst.* **19**, 885 (2010).
6. M.J. Williamson, R.M. Tromp, P.M. Vereecken, F.M. Ross, *Nat. Mater.* **2**, 532 (2003).
7. A.J. Leenheer, J.P. Sullivan, M.J. Shaw, C.T. Harris, *J. Microelectromech. Syst.* **24**, 1061 (2015).
8. R.R. Unocic, R.L. Sacci, G.M. Brown, G.M. Veith, N.J. Dudney, K.L. More, F.S. Walden, 2nd, D.S. Gardiner, J. Damiano, D.P. Nackashi, *Microsc. Microanal.* **20**, 452 (2014).
9. E. Fahrenkrug, D.H. Alsem, N. Salmon, S. Maldonado, *J. Electrochem. Soc.* **164**, H358 (2017).
10. R. Girod, N. Nianias, V. Tileli, *Microsc. Microanal.* **25**, 1304 (2019).
11. A. Radisic, P.M. Vereecken, J.B. Hannon, P.C. Searson, F.M. Ross, *Nano Lett.* **6**, 238 (2006).
12. A. Radisic, P.M. Vereecken, P.C. Searson, F.M. Ross, *Surf. Sci.* **600**, 1817 (2006).
13. J. Yang, C.M. Andrei, Y. Chan, B.L. Mehdi, N.D. Browning, G.A. Botton, L. Soleymani, *Langmuir* **35**, 862 (2019).
14. J. Yang, C.M. Andrei, G.A. Botton, L. Soleymani, *J. Phys. Chem. C* **121**, 7435 (2017).
15. X. Chen, K.W. Noh, J.G. Wen, S.J. Dillon, *Acta Mater.* **60**, 192 (2012).
16. E.R. White, S.B. Singer, V. Augustyn, W.A. Hubbard, M. Mecklenburg, B. Dunn, B.C. Regan, *ACS Nano* **6**, 6308 (2012).
17. M. Sun, H.G. Liao, K. Niu, H. Zheng, *Sci. Rep.* **3**, 3227 (2013).
18. J.H. Park, N.M. Schneider, D.A. Steingart, H. Deligianni, S. Kodambaka, F.M. Ross, *Nano Lett* **18**, 1093 (2018).
19. J.B. Goodenough, Y. Kim, *Chem. Mater.* **22**, 587 (2010).
20. A.J. Leenheer, K.L. Jungjohann, K.R. Zavadil, J.P. Sullivan, C.T. Harris, *ACS Nano* **9**, 4379 (2015).
21. L. Lutz, W. Dachraoui, A. Demortière, L.R. Johnson, P.G. Bruce, A. Grimaud, J.-M. Tarascon, *Nano Lett.* **18**, 1280 (2018).
22. M. Gu, L.R. Parent, B.L. Mehdi, R.R. Unocic, M.T. McDowell, Robert L. Sacci, W. Xu, J.G. Connell, P. Xu, P. Abellan, X. Chen, Y. Zhang, D.E. Perea, J.E. Evans, L.J. Lauhon, J.-G. Zhang, J. Liu, N.D. Browning, Y. Cui, I. Arslan, C.-M. Wang, *Nano Lett.* **13**, 6106 (2013).
23. R.R. Unocic, X.G. Sun, R.L. Sacci, L.A. Adamczyk, D.H. Alsem, S. Dai, N.J. Dudney, K.L. More, *Microsc. Microanal.* **20**, 1029 (2014).
24. Z. Zeng, X. Zhang, K. Bustillo, K. Niu, C. Gamme, J. Xu, H. Zheng, *Nano Lett.* **15**, 5214 (2015).
25. Z. Zeng, W.-I. Liang, Y.-H. Chu, H. Zheng, *Faraday Discuss.* **176**, 95 (2014).
26. Z. Zeng, W.-I. Liang, H.-G. Liao, H.L. Xin, Y.-H. Chu, H. Zheng, *Nano Lett.* **14**, 1745 (2014).
27. R.L. Sacci, N.J. Dudney, K.L. More, L.R. Parent, I. Arslan, N.D. Browning, R.R. Unoci, *Chem. Commun.* **50**, 2104 (2014).
28. R.L. Sacci, J.M. Black, N. Balke, N.J. Dudney, K.L. More, R.R. Unocic, *Nano Lett.* **15**, 2011 (2015).
29. B.L. Mehdi, J. Qian, E. Nasybulin, C. Park, D.A. Welch, R. Faller, H. Mehta, W.A. Henderson, W. Xu, C.M. Wang, J.E. Evans, J. Liu, J.G. Zhang, K.T. Mueller, N.D. Browning, *Nano Lett.* **15**, 2168 (2015).
30. R.L. Sacci, J.M. Black, N. Balke, N.J. Dudney, K.L. More, R.R. Unocic, *Nano Lett.* **15**, 2011 (2015).
31. A.J. Leenheer, K.L. Jungjohann, K.R. Zavadil, J.P. Sullivan, C.T. Harris, *ACS Nano* **9**, 4379 (2015).
32. K.L. Harrison, K.R. Zavadil, N.T. Hahn, X. Meng, J.W. Elam, A. Leenheer, J.-G. Zhang, K.L. Jungjohann, *ACS Nano* **11**, 11194 (2017).
33. A. Kushima, K.P. So, C. Su, P. Bai, N. Kuriyama, T. Maebashi, Y. Fujiwara, M.Z. Bazant, J. Li, *Nano Energy* **32**, 271 (2017).
34. B.L. Mehdi, A. Stevens, J. Qian, C. Park, W. Xu, W.A. Henderson, J.G. Zhang, K.T. Mueller, N.D. Browning, *Sci. Rep.* **6**, 34267 (2016).
35. Y. Li, Y. Li, A. Pei, K. Yan, Y. Sun, C.-L. Wu, L.-M. Joubert, R. Chin, A.L. Koh, Y. Yu, J. Perrino, B. Butz, S. Chu, Y. Cui, *Science* **358**, 506 (2017).
36. M.J. Zachman, Z. Tu, S. Choudhury, L.A. Archer, L.F. Kourkoutis, *Nature* **560**, 345 (2018).
37. A. Kushima, T. Koido, Y. Fujiwara, N. Kuriyama, N. Kusumi, J. Li, *Nano Lett.* **15**, 8260 (2015).
38. O.M. Karakulina, A. Demortière, W. Dachraoui, A.M. Abakumov, J. Hadermann, *Nano Lett.* **18**, 6286 (2018).
39. M.E. Holtz, Y. Yu, D. Gunceler, J. Gao, R. Sundararaman, K.A. Schwarz, T.s.A. Arias, Héctor D. Abruña, D.A. Muller, *Nano Lett.* **14**, 1453 (2014).
40. N. Hodnik, G. Dehm, K.J. Mayrhofer, *Acc. Chem. Res.* **49**, 2015 (2016).
41. G.-Z. Zhu, S. Prabhudev, J. Yang, C.M. Gabardo, G.A. Botton, L. Soleymani, *J. Phys. Chem. C* **118**, 22111 (2014).

42. V. Beermann, M.E. Holtz, E. Padgett, J.F. de Araujo, D.A. Muller, P. Strasser, *Energy Environ. Sci.* **12**, 2476 (2019).
43. D.M. Bastidas, *Metals* **10**, 458 (2020).
44. A. Kosari, H. Zandbergen, F. Tichelaar, P. Visser, H. Terryn, A. Mol, *Corrosion* **76**, 4 (2020).
45. S. Chee, R. Hull, F. Ross, *Microsc. Microanal.* **18**, 1110 (2012).
46. S.W. Chee, D.J. Duquette, F.M. Ross, R. Hull, *Microsc. Microanal.* **20**, 462 (2014).
47. S.W. Chee, S.H. Pratt, K. Hattar, D. Duquette, F.M. Ross, R. Hull, *Chem. Commun.* **51**, 168 (2015).
48. D. Gross, J. Kacher, J. Key, K. Hattar, I.M. Robertson, *Processing, Properties, and Design of Advanced Ceramics and Composites II* **261**, 329 (2017).
49. J.W. Key, S. Zhu, C.M. Rouleau, R.R. Unocic, Y. Xie, J. Kacher, *Ultramicroscopy* **209**, 112842 (2020).
50. S. Malladi, C. Shen, Q. Xu, T. de Kruijff, E. Yücelen, F. Tichelaar, H. Zandbergen, *Chem. Commun.* **49**, 10859 (2013).
51. S. Schilling, A. Janssen, N.J. Zaluzec, M.G. Burke, *Microsc. Microanal.* **23**, 741 (2017).
52. S.C. Hayden, C. Chisholm, R.O. Grudt, J.A. Aguiar, W.M. Mook, P.G. Kotula, T.S. Pilyugina, D.C. Bufford, K. Hattar, T.J. Kucharski, I.M. Taie, M.L. Ostraat, K.L. Jungjohann, *NPJ Mater. Degrad.* **3**, 1 (2019).
53. K. Gao, W. Chu, B. Gu, T. Zhang, L. Qiao, *Corrosion* **56**, 515 (2000).
54. S. Bhowmick, H. Espinosa, K. Jungjohann, T. Pardoen, O. Pierron, *MRS Bull.* **44**, 487 (2019).
55. B.B. Lewis, M.G. Stanford, J.D. Fowlkes, K. Lester, H. Plank, P.D. Rack, *Beilstein J. Nanotechnol.* **6**, 907 (2015).
56. A.J. Leenheer, K.L. Jungjohann, C.T. Harris, *Microsc. Microanal.* **21**, 1293 (2015).
57. J.L. Hart, A.C. Lang, A.C. Leff, P. Longo, C. Trevor, R.D. Twesten, M.L. Taheri, *Sci. Rep.* **7**, 1 (2017).
58. N.M. Schneider, M.M. Norton, B.J. Mendel, J.M. Grogan, F.M. Ross, H.H. Bau, *J. Phys. Chem. C* **118**, 22373 (2014).
59. T.J. Woehl, P. Abellan, *J. Microsc.* **265**, 135 (2017).
60. T.J. Woehl, K.L. Jungjohann, J.E. Evans, I. Arslan, W.D. Ristenpart, N.D. Browning, *Ultramicroscopy* **127**, 53 (2013).
61. P. Abellan, B.L. Mehdi, L.R. Parent, M. Gu, C. Park, W. Xu, Y. Zhang, I. Arslan, J.-G. Zhang, C.-M. Wang, J.E. Evans, N.D. Browning, *Nano Lett.* **14**, 1293 (2014).
62. E.A. Sutter, P.W. Sutter, *J. Am. Chem. Soc.* **136**, 16865 (2014).
63. K. Karki, T. Mefford, D.H. Alsem, N. Salmon, W.C. Chueh, *Microsc. Microanal.* **24**, 324 (2018).
64. E.A. Stricker, X. Ke, J.S. Wainright, R.R. Unocic, R.F. Savinell, *J. Electrochem. Soc.* **166**, H126 (2019).
65. B.L. Mehdi, A. Stevens, L. Kovarik, N. Jiang, H. Mehta, A. Liyu, S. Reehl, B. Stanfill, L. Luzi, W. Hao, L. Bramer, N.D. Browning, *App. Phys. Lett.* **115** 063102 (2019).
66. B.H. Kim, J. Heo, S. Kim, C.F. Reboul, H. Chun, D. Kang, H. Bae, H. Hyun, J. Lim, H. Lee, B. Han, T. Hyeon, A.P. Alivisatos, P. Ercius, H. Elmlund, J. Park, *Science* **368**, 60 (2020).
67. M.J. Zachman, J.A. Hachtel, J.C. Idrobo, M. Chi, *Angew. Chem. Int. Ed.* **59**, 1384 (2020). □

Raymond Unocic is a senior staff scientist at the Center for Nanophase Materials Sciences (CNMS) at Oak Ridge National Laboratory. He is the theme science leader for the Directed Nanoscale Transformation theme at CNMS and past leader of the Microscopy Society of America's Focused Interest Group on Electron Microscopy in Liquids and Gases. His research focuses on the development and application of *in situ* microscopy methods to probe dynamic processes in energy storage materials, 2D materials, catalysts, and structural materials. He has received Oak Ridge National Laboratory's Alvin M Weinberg distinguished fellowship, Microanalysis Society's Birks Award, and the R&D 100 Award. Unocic can be reached by email at unocicrr@ornl.gov.

Katherine Jungjohann is a staff scientist at the Center for Integrated Nanotechnologies (CINT) at Sandia National Laboratories. She is the thrust leader for the In Situ Characterization and Nanomechanics Thrust at CINT, and the co-leader of the Microscopy Society of America's Focused Interest Group on Electron Microscopy in Liquids and Gases. Her research includes developing new capabilities for *in situ* TEM imaging of environmentally relevant materials processes, with a current focus on energy-storage interfaces and corrosion mechanisms. Jungjohann can be reached by email at kljungj@sandia.gov.

B. Layla Mehdi is an assistant professor and associate director of the Albert Crewe Center for Electron Microscopy at the University of Liverpool, UK. Her research focuses on the development of *operando* electrochemical electron microscopy capabilities, emphasizing energy storage, electrocatalysis, and pharmaceutical applications in both liquids and gases. She has received the Microscopy Society of America Early Career Albert Crewe Award, a Materials Research Society Postdoctoral Award, a Japan Society for the Promotion of Science fellowship, a Microscopy and Microanalysis Presidential Award, and the Robert P. Apkarian Award for her development of *operando* measurements for beam-sensitive materials, including Li-ion batteries. Mehdi can be reached by email at b.l.mehdi@liverpool.ac.uk.

Nigel Browning is the director of the Albert Crewe Center for Electron Microscopy at the University of Liverpool, UK. He is the chair of the 2022 Gordon Research Conference on Liquid Phase Electron Microscopy. His research focuses on the development of new high spatial, temporal, and energy-resolution methods in electron microscopy. He is a Fellow of the American Association for the Advancement of Science and the Microscopy Society of America (MSA). Throughout his career, he has received the Burton Award (MSA), the Coble Award (American Ceramic Society), the R&D 100 Award, the Nano 50 Award, and the Microscopy Today Innovation Award. Browning can be reached at nigel.browning@liverpool.ac.uk.

Chongmin Wang is a laboratory Fellow at Pacific Northwest National Laboratory (PNNL). Before Joining PNNL, he worked at the Max-Planck Institute for Metal Research, Germany, NIMS, Japan, and Lehigh University. His research focuses on advanced microscopy, specifically *in situ* microscopy and energy materials. His awards include the Materials Research Society's (MRS) Innovation in Materials Characterization Award, the Microscopy Today Innovation Award, the Rowland Snow Award (American Ceramic Society), the R&D100 Award, a *JMR* Paper of the Year Award (MRS), the Outstanding Invention Award (Japan), and the PNNL Directors Award for Exceptional Scientific Achievement. He is a Fellow of the Materials Research Society. Wang can be reached by email at Chongmin.wang@pnnl.gov.